Waveguide Hyperthermia Applicator with Circular Polarisation

I. Merunka, O. Fiser, L. Vojackova, and J. Vrba
Department of Electromagnetic Field, Czech Technical University in Prague, Czech Republic

Abstract— We dedicated this contribution to design of a circular waveguide microwave hyperthermia applicator with circular polarisation. Designing equations as well as optimization process of applicator using numerical simulator of electromagnetic field are described. Numerical simulations of specific absorption rate (SAR) and consecutive thermal simulation confirmed our assumption, that a spherical object can be better covered by SAR with an applicator with circular polarisation.

1. INTRODUCTION

We present a circular waveguide applicator with circularly polarized wave at its aperture in this contribution. There is a lot of ways how to improve success rate of cancer treatment. One of these is hyperthermia [1]. The main idea of hyperthermia is to raise the temperature in a tumour to the specific level and for a period of time, which causes the cell death or higher sensitivity to ionizing radiation or chemotherapy [2]. In our previous contributions we studied UWB antenna and its application to microwave hyperthermia [3]. There we observed polarization of dielectric on the interface between spherical phantom of tumour and phantom of human breast in numerical simulations. This phenomenon causes hotpots on the interface between the tumour and surrounding tissue, while the temperature inside of the tumour does not even reach the therapeutic level. Using of a circularly polarized hyperthermia applicator could at least partially solve this issue.

2. MATERIALS AND METHODS

2.1. Configuration of Numerical Experiment

The circular waveguide hyperthermia applicator was facing to the water bolus of thickness of 2 cm with dielectric parameters of $\varepsilon_{rel} = 78.0$, $\sigma = 0.04\,\mathrm{S/m}$ followed by human breast phantom with average dielectric parameters of $\varepsilon_{rel} = 10.0$, $\sigma = 0.16\,\mathrm{S/m}$. Human breast phantom has shape of brick and size of $130 \times 200 \times 200$ mm. The applicator was optimized to work well in this configuration. Then a spherical numerical phantom of tumour ($\varepsilon_{rel} = 49.9$, $\sigma = 0.79\,\mathrm{S/m}$) with radius of 1 cm was inserted 0.5 cm under the breast phantom surface to compare the applicators performance. This configuration in two different cross–sections can be seen in Figure 1.

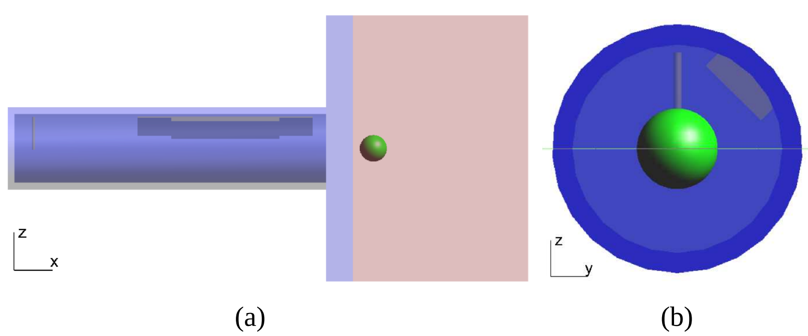

Figure 1: Configuration of numerical model. (a) y-cross-section, (b) x-cross-section.

2.2. Electromagnetic Simulation

The applicator was designed to operate well on frequency 434 MHz. This frequency was chosen with respect to the size of a heated region, size of the antenna, effective penetration depth, ISM frequency bands (Europe) and working frequency of microwave power generators usually used in field of microwave hyperthermia. Numerical simulations of electromagnetic (EM) field of numerical model was computed using 3D full-wave electromagnetic and thermal simulation platform SEMCAD X (Schmid & Partner Engineering AG, Zurich).

2.3. Thermal Simulation

We also computed thermal distribution in the heated region after the EM simulation. We used steady state solver, which implements Penne's bioheat equation. Thermal tissue parameters were taken from the IT'IS foundation material database [4] and are listed in Table 1. Initial temperature of all the tissues were set to 37°C, temperature of the water surrounding the breast phantom was set to 25°C. We consider constant heat generation rate and constant heat transfer rate in the tissues. Thermal boundary was inserted between the water and the neck phantom. The value of the heat transfer coefficient of this boundary is taken from [5] and set to 65 W/m^2/K. SAR distribution from EM simulation was used as the heat source.

Table 1: Human breast phantom parameters used in numerical simulations.

Density (kg/m)	Specific Heat Capacity (J/kg/K)	Thermal Conductivity (W/m/K)	Heat Generation Rate (W/kg)	Heat Transfer Rate (W/m^3/K)
984.3	2654.2	0.272	1.526	6548.7

2.4. Applicator Design

To design the circular waveguide we need to determine only its radius a with respect to dielectric material inside the waveguide, mode and working frequency. In this case, the waveguide is filled by distilled water ($\varepsilon_{rel} = 78$, $\sigma = 0.04$ S/m), desired mode is dominant mode TE$_{11}$ and operating frequency 434 MHz. Than radius a can be calculated according to simple equation [6]:

$$a = \frac{p_{11}}{2\pi f_{c_{11}} \sqrt{\mu\varepsilon}} \tag{1}$$

where value of p_{11} equals to 1.841, μ and ε has meaning of permeability and permittivity and $f_{c_{11}}$ has meaning of cut off frequency of desired mode. Cut off frequency was set to 380 MHz, so the frequency 434 MHz was approximately in the middle of the interval between the cut off frequency of TE$_{11}$ mode and the second closest TM$_{01}$ mode ($f_{c_{01}} = 496$ MHz). Finally, diameter $2a$ of the waveguide was computed to 5.17 cm.

Polarization plate was than inserted into the waveguide. Its size and position was taken from [7], where the metal fin was introduced into the circular waveguide working on wavelength of 1.25 cm. Dimensions of the fin was adapted with respect to the wavelength in our waveguide. Applicator has length of 23.1 cm.

Feeding of the antenna was realized using a power probe. Its length and position was established during the optimization procedure. Best results were achieved with length of the probe 25 mm and distance of 14 mm from the short (rear inner part of the applicator). Perfect electric conductor was set as the material of the fin, the probe and the whole applicator in numerical model.

3. RESULTS

In Figure 2 can be seen waveform of the absolute value of reflection coefficient. The applicator is well matched, value of the reflection coefficient is less than −18 dB on frequency 434 MHz.

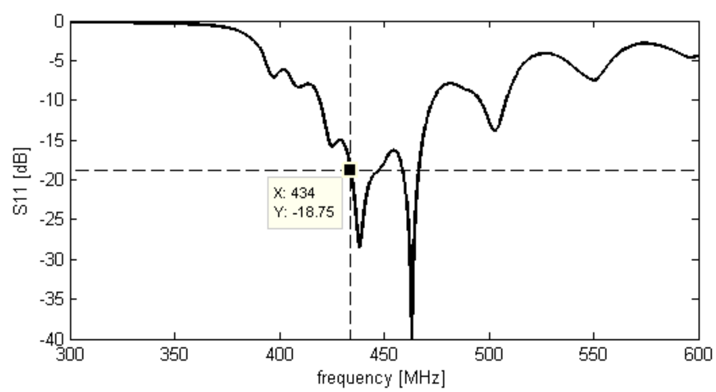

Figure 2: Impedance matching of the applicator.

Specific absorption rate in the cross section of the tumour is depicted in Figures 3(a), 3(b). There is a comparison between the SAR obtained by applicator with the polarizer and without the polarizer. Applicator with circularly polarized field made possible to cover the tumour by SAR from all directions partially. SAR is distributed more diffuse on the boundary and its values are higher inside the tumour. Extreme hotspots in the direction of applicator polarization did not completely disappeared, because the new applicator does not create absolutely circularly polarized E-field.

Effective penetration depth (EPD) defined as distance between the point of the entrance of electromagnetic wave into the breast phantom and point where value of SAR decreases to 25% of its maximal value was also compared in both cases. EPD with the waveguide without polariser equals to 1.8 cm, EPD with waveguide with circular polarisation equals to 1.7 cm, which is almost the same value.

In results from thermal simulations can be seen more uniform temperature distribution in the case with circularly polarised wave. Extreme values in positions of SAR hotspots are suppressed and phantom of tumour is heated along its boundary well. However temperature in the middle of the tumour is almost the same in both cases.

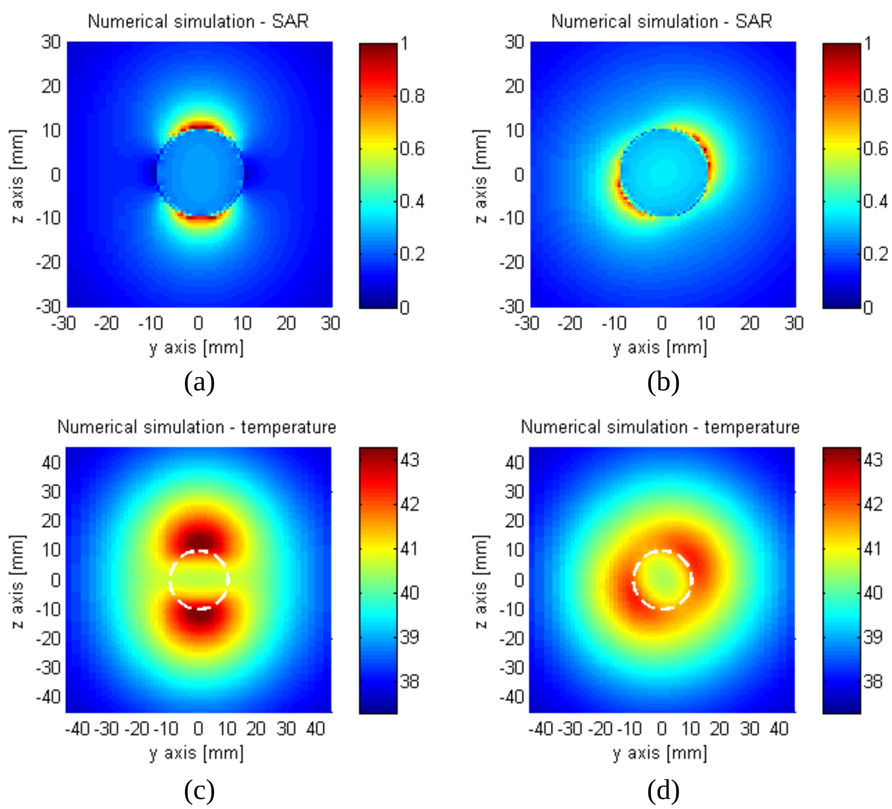

Figure 3: SAR [W/kg] and temperature [°C] distribution in the cross section of the tumour phantom. (a) and (c) without polarizer, (b) and (d) with polarizer.

4. CONCLUSION

In this contribution we designed microwave hyperthermia applicator with circular polarisation. Results of the numerical simulations of SAR and temperature distribution confirmed, that circular objects could be heated more uniformly at least in the cross section perpendicular to main axis of applicator. On the other hand, the effective penetration depth decreased relatively to the rectangular waveguide applicators. The ability of focusing microwave power by using a multi-antenna array is also limited.

ACKNOWLEDGMENT

This study was supported by the COST Action TD1301: "Development of a European-based Collaborative Network to Accelerate Technological, Clinical and Commercialization Progress in the Area of Medical Microwave Imaging" as well as students project SGS 2014, with number SGS14/189/OHK3/3T/13: "Interactions of EM field with biological systems and theirs applications in medicine".

REFERENCES

1. Wust, P., B. Hildebrandt, G. Sreenivasa, B. Rau, J. Gellermann, H. Riess, R. Felix, and P. Schlag, "Hyperthermia in combined treatment of cancer," *The Lancet Oncology*, Vol. 3, No. 8, 487–497, Aug. 2002.
2. Trefna, H. D., J. Vrba, and M. Persson, "Time-reversal focusing in microwave hyperthermia for deep-seated tumors," *Phys. Med. Biol.*, Vol. 55, No. 8, 2167, Apr. 2010.
3. Merunka, I., O. Fiser, L. Vojackova, J. Vrba, and D. Vrba, "Utilization potential of balanced antipodal Vivaldi antenna for microwave hyperthermia treatment of breast cancer," *2014 8th European Conference on Antennas and Propagation (EuCAP)*, 706–710, 2014.
4. Hasgall, P. A., F. Di Gennaro, C. Baumgartner, E. Neufeld, M. C Gosselin, D. Payne, A. Klingenbckk, and N. Kuster, "ITIS database for thermal and electromagnetic parameters of biological tissues," Version 2.6, Jan. 13, 2015.
5. Boutelier, C., L. Bougues, and J. Timbal, "Experimental study of convective heat transfer coefficient for the human body in water," *Journal of Applied Physiology: Respiratory, Environmental and Exercise Physiology*, Vol. 42, No. 1, 93–100, Jan. 1977.
6. Pozar, D. M., *Microwave Engineering*, 4th Edition, Wiley, Hoboken, NJ, 2011.
7. Montgomery, C. G., R. H. Dicke, and E. M. Purcell, Eds., *Principles of Microwave Circuits*, New Edition, The Institution of Engineering and Technology, London, UK, 1986.